REDVET - Revista electrónica de Veterinaria - ISSN 1695-7504
Vol 25, No. 2 (2024)
http://www.veterinaria.org
Article Received: 20.10.2024 Revised: 09.11.2024 Accepted: 08.12.2024

Biosynthesized Zinc Oxide Nanoparticles from *Herdmania pallida*: Structural, Optical, Antioxidant, and Antibacterial Studies

V.Priya[1], S.Sankaravadivu[1*],J.Mukila[2]

[1]Research Scholar(Reg.No 241120114010), [1,1*,2] PG & Research Department of Chemistry, A.P.C. Mahalaxmi College for Women, Thoothukudi.Affiliated to Manonmaniam Sundaranar University, Abishekapatti, Tirunelveli-627012, Tamil Nadu, India.

Abstract:
Nanotechnology deals with the production and application of materials with nanoscale dimensions. The nanoscale size provides nanoparticles with a high surface area to volume ratio, resulting in unique physicochemical properties. Biosynthesis of nanoparticles is an important area in nanotechnology due to its eco-friendly and cost-effective advantages over conventional chemical and physical synthesis methods. The present study focuses on the biosynthesis of zinc oxide nanoparticles (ZnO NPs) using ethanolic extract of the simple ascidian Herdmania pallida as a reducing and stabilizing agent. The synthesis of ZnO nanoparticles was confirmed using UV–Visible spectroscopy, Fourier Transform Infrared Spectroscopy (FTIR), X-ray Diffraction (XRD), Scanning Electron Microscopy (SEM), and Energy Dispersive X-ray Analysis (EDX). The synthesized nanoparticles were further applied as photocatalysts for the degradation of methylene blue (MB) dye under ultraviolet (UV) light irradiation. The results demonstrated that the degradation efficiency strongly depended on UV illumination time and the concentration of ZnO nanoparticles. The photocatalytic degradation reaction followed pseudo-first-order kinetics with respect to dye concentration. Cyclic Voltammetry (CV) analysis was employed to investigate the electrochemical and redox behavior of the ZnO nanoparticles. The antioxidant activity of ZnO NPs was evaluated using DPPH free radical scavenging and hydrogen peroxide (H_2O_2) scavenging assays at different concentrations, which revealed significant antioxidant potential. In addition, the antibacterial activity of the synthesized ZnO nanoparticles was investigated against bacterial strains such as Escherichia coli, Staphylococcus aureus, and Pseudomonas aeruginosa, demonstrating effective antibacterial activity. The study highlights the potential application of marine-derived biosynthesized ZnO nanoparticles in environmental and biomedical fields.

Keywords: Antibacterial Activity, Antioxidant Acitivity, Catalytic Activity, *Herdmania pallida*, ZnO NPs, .

1. **Introduction:**

Nanotechnology is emerging as a rapidly growing field with its application in science and technology for the purpose of manufacturing new materials at the nanoscale level [1]. Nanotechnology has drawn more attention for its cutting-edge nature and wide application range in almost every field of science and technology, including biomedical sciences [2, 3]. Nanomaterials are of great importance because of their superior physicochemical and biological properties over their bulk phase. The size of these nanostructured materials (1–100 nm) offers a higher surface -to-volume ratio, which leads to high surface reactivity. [4]

Ascidians are marine sedentary organisms, and they belong to the biofouling community. They are found in piers, pilings, harbor installations, materials used in aquaculture operations, etc. *Herdmania pallida* is a simple ascidian belonging to the family Ascidiidae. Ascidians are consumed as food in many parts of the world, and there are coastal aquafarms in Japan as well as Thailand for the culture of ascidians. *Microcosmus sulcatus*, *Styela plicata,* and *Polycarpa pomaria* are taken as food in the Mediterranean [5]. Ascidians (Chordata, Ascidiacea) are sessile filter-feeding organisms closely related to vertebrates [6], able to filter even minute particulate matter [7, 8]. They are well known for their ability to accumulate heavy metals [9, 10] and to thrive in eutrophic (nutrient-rich) and polluted environments. There are nearly 3000 species of ascidians inhabiting all marine habitats from shallow water to the deep sea, with some species, in particular invasive species, creating large aggregations on artificial structures [11, 12]. They occur as the major components of a fouling community settling on all kinds of surfaces: hard rocks, stone, the hull of ships, branches and roots of trees, algae, floating objects, sand, and muddy surfaces [13, 14]. Marine organisms contain a significant amount of carbohydrates, proteins, and lipids, which are essential for human beings [15]. There are more and more reports on the production of nanoparticles from biologically derived materials such as plants, algae, fungi, bacteria, and animals [16].

ZnONPs, which can exhibit a wide variety of nanostructures, are believed to be biosafe, nontoxic, and biocompatiable and have been used in various technologies and industries such as optoelectronics, piezoelectric and magnetic sensors, biodiagnosis, biological labelling, ceramic and rubber processing, environmental protection, biology, and the medicinal industry [17-19]. Zinc oxide (ZnO), an important semiconductor nanoparticle, has been attracting attention for its wide range of applications, such as electronics, optics, optoelectronics, and biomedicine [20]. Nanoparticles can be generated from various materials in numerous shapes, such as wires, spheres, tubes, and rods [21, 22]. Zinc oxide (ZnO) has fascinated several researchers from different disciplines of science due to its wide applications and unique

REDVET - Revista electrónica de Veterinaria - ISSN 1695-7504
Vol 25, No. 2 (2024)
http://www.veterinaria.org
Article Received: 20.10.2024 Revised: 90.11.2024 Accepted: 08.12.2024

characteristics [23]. ZnO is referred to has received great consideration in striking electronic applications because of its unique chemical, optical, and electrical features [24]. The present study aims to synthesize ZnO NPs using *Herdmania pallida.* Recent research also focused on the synthesized sample, which was characterized using Fourier transform infrared spectroscopy (FT-IR), UV–visible spectroscopy, scanning electron microscopy (SEM) and energy dispersive X-ray (EDX), electrochemical studies, photocatalytic properties (particularly in dye degradation), and antioxidant properties.

2. Materials and Methods:

2.1. Collection of Sample:

Herdmania pallida samples were collected directly from the sea by handpicking from rocks and submerged surfaces in the intertidal region in Thoothukudi during the month of February 2024, A survey was subsequently undertaken by SCUBA diving along the shore of the harbor in order to map the distribution of the species, with searches focused at eight sites within the harbor. A specimen was deposited in the Museum of the Department of Zoology, A.P.C. Mahalaxmi College for Women, Tuticorin 628002, Tamil Nadu, India.

Fig.1 *Herdmania pallida*

2.2 SYNTHESIS OF ZINC OXIDE NANOPARTICLES

2.2.1. Preparation of Sample:

The collected samples were rinsed with sterile seawater to remove associated debris and salt. Ten grams of the sample were weighed and preserved separately in an ethanol mixture (1:2) and brought to the laboratory, and the extract was filtered using filter paper and used for further studies.

2.2.2. Preparation of Zinc Sulphate:

Zinc Sulphate ($ZnSO_4$) analytical grade was purchased from Merck & Co. and used without further purification. Double-distilled deionized (DI) water was used throughout the course of this investigation. Whatman No.1 filter paper was used for filtration. A solution of $ZnSO_4$ was prepared by dissolving the solid $ZnSO_4$ in DI water.

2.2.3. Preparation of ZnO NPs

ZnO NPs were produced from the *Herdmania pallida* using 0.01 M $ZnSO_4.7H_2O$ and 0.1 N NaOH as precursors [25]. It was added dropwise to maintain pH at 8, then the mixture was stirred and heated at 70°C for 30 min for complete reduction and formation of a white precipitate. The resulting material was then collected via decantation, washed with distilled water to remove residuals, and oven-dried overnight at 70°C to yield powdered ZnO nanoparticles [26, 27, 28]

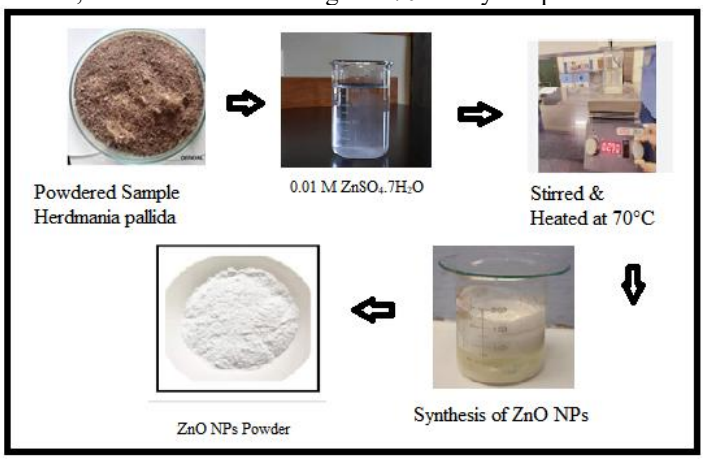

Fig. 2 Synthesis of ZnO Powder

REDVET - Revista electrónica de Veterinaria - ISSN 1695-7504
Vol 25, No. 2 (2024)
http://www.veterinaria.org
Article Received: 20.10.2024 Revised: 90.11.2024 Accepted: 08.12.2024

3. **CHARACTERIZATION:**
The use of various analytical techniques, such as UV-visible spectrophotometry, XRD, SEM, EDX, and FTIR, analysis, in the characterization of biosynthesized ZnO NPs has been extensively reported in this literature. These techniques provide valuable information on the physical and chemical properties of nanoparticles, including their size, shape, surface charge, crystallinity, and surface functional groups, for instance.

3.1. UV-Visible Spectroscopy:
The optical properties and formation of biosynthesized zinc oxide nanoparticles (ZnO NPs) were analyzed using UV–Visible spectroscopy. The synthesized ZnO nanoparticles were dispersed in distilled water and sonicated to obtain a uniform suspension. The prepared sample was transferred into a quartz cuvette, and the absorption spectrum was recorded using a UV–Visible spectrophotometer in the wavelength range of 200–800 nm. Distilled water was used as the blank solution for baseline correction. The appearance of a characteristic absorption peak in the UV region confirmed the formation of ZnO nanoparticles due to surface plasmon resonance and electronic transitions. The obtained absorption data were further used to determine the optical properties and band gap energy of the synthesized nanoparticles.

3.2 XRD Analysis:
X-ray diffraction (XRD) analysis of the synthesized ZnO nanoparticles was performed using an X-ray diffractometer with Cu-Kα radiation (λ = 1.5406 Å) operated at 40 kV and 30 mA. Scanning was carried out over a 2θ range of 10° to 80° at a rate of 2°/min. XRD analysis enables accurate phase identification, estimation of crystallite size, and structural characterization of the nanoparticles.XRD analysis provides information on the crystalline structure and phase purity of nanoparticles. The crystal size of the biosynthesized ZnONPs is generally calculated on the basis of XRD analysis [29].

3.3 SEM and EDX Analysis:
The morphology, size, and elemental composition of the synthesized ZnO nanoparticles were examined using scanning electron microscopy (SEM) coupled with energy-dispersive X-ray (EDX) analysis (Hitachi 4160). SEM provided detailed information on particle shape and surface features, while EDX confirmed the presence of the constituent elements in the nanoparticles.

3.4 Fourier Transform Infrared Spectroscopy (FT-IR):
The FT-IR spectra of the nanoparticles were recorded using a Fourier Transform Infrared Spectrometer (Thermo Scientific Nicolet iS5 iD5) equipped with a ZnSe (zinc selenide) ATR/Attenuated Total Reflectance accessory. FT-IR spectroscopy was employed to identify the functional groups present on the surface of the ZnO nanoparticles.

3.5 Electrochemical Study:
From cyclic voltammetry studies, the working electrodes were prepared by grinding the combination of 70% prepared ZnO powder, 20% graphite, and two drops of silicone oil used as a binder and subsequently pasting on a disk electrode. A platinum foil was used as a counter electrode, an Ag/AgCl electrode, as a reference electrode and a 3M KOH solution as an electrolyte.[30]

3.6 **Photocatalytic degradation of MB dye by ZnO NPs :**
The photocatalytic degradation of MB dye by ZnO NPs was assessed under natural sunlight irradiation. All the experiments were conducted in a glass container consisting of 100 mL of 20 ppm MB dye with 50 mg of ZnO NPs, magnetically stirred under sunlight irradiation. Before irradiation, the contents were magnetically agitated in the dark for thirty min to accomplish adsorption–desorption equilibrium between dye and ZnO NPs. During the process, the samples were withdrawn and centrifuged, and the dye concentration was monitored by checking the absorbance at 662 nm.
The degradation of MB dye was fitted to a pseudo-first-order reaction and given by $-\ln(Ao-At) = -Kt$ (1), where Ao and At are the initial and final concentrations of MB (ppm) after sunlight irradiation, td is the time required for photocatalytic degradation (min), and kd is the photocatalytic degradation constant (min^{-1}). [31]

4. Application:
4.1. Antioxidant Activity of Synthesized Nanoparticles:
A. DPPH radical scavenging activity:
The free radical scavenging activity of the synthesized nanoparticles of zinc oxide on the stable radical 2,2-diphenyl-2-picrylhyrazyl (DPPH) was estimated [32]. Synthesized nanoparticles of aqueous ascidian extracts at different concentrations (12.5, 25, 50, 100, and 200 g/mL) were incubated with 3.0 mL of a DPPH methanol solution (0.1 mM) in the dark for 30 min at room temperature, followed by measuring the absorbance at 517 nm using a UV-Vis spectrophotometer (Genesys 10s UV: Thermo Electron Corporation). Ascorbic acid was used as the reference standard. The capability to scavenge the DPPH radical was calculated by using the following formula. DPPH radical scavenging

REDVET - Revista electrónica de Veterinaria - ISSN 1695-7504
Vol 25, No. 2 (2024)
http://www.veterinaria.org
Article Received: 20.10.2024 Revised: 90.11.2024 Accepted: 08.12.2024

effect = $(A_0 - A_1)/A_0$ □ 100 % inhibition Where A_0 is the absorbance of the control, and A_1 is the absorbance of the test samples and reference. All the tested samples were performed in triplicate, and the results were averaged.

B. Hydrogen peroxide radical scavenging activity:
As per the method [33], the hydrogen peroxide (H_2O_2) scavenging ability of the synthesized ascorbic acid nanoparticles was established. In phosphate buffer (pH 7.4), a solution of H_2O_2 (40mM) was arranged. Dissimilar concentrations (12.5, 25, 50, 100, and 200 µg/mL) of nanoparticles of ascorbic acid in 3.4 ml phosphate buffer were added. These are added to the H_2O_2 solution (0.6 ml, 40 mM). At 230 nm, the absorbance value of the reaction mixture was recorded. Using equation (1) as mentioned above, the percentage of H_2O_2 scavenging activity was calculated.

4.2 Antibacterial Activity:
The test bacteria was inoculated in peptone water and incubated for 3 – 4 hours at 35 ºC. Mueller hinton agar plates was prepared and poured in sterile petriplates. 0.1 ml of bacterial culture was inoculated on the surface of Mueller hinton agar plates and spread by using L-rod. The inoculated plates was allowed to dry for five minutes. The disk loaded with samples concentration 1000 µg/ml was placed on the surface of inoculated petriplates using sterile technique. The plate was incubated at 37 ºC for 18-24 hours. The plate was examined for inhibitory zone and the zone of inhibition was measured in mm[34]

5. RESULT AND DISCUSSION:
5.1 UV-Visible spectrophotometric analysis:
The UV–visible spectrophotometric analysis of the synthesized Zinc Oxide nanoparticles is shown in Fig. 3(a). The UV–visible spectra of ZnO nanoparticles synthesized using the aqueous extract of *Herdmania pallida* exhibited a strong absorption peak at 380 nm, confirming the formation of ZnO nanoparticles. This absorption band is attributed to the electron transition from the valence band to the conduction band, which is a characteristic feature of ZnO nanomaterials.The absorption peak around 380 nm corresponds to the intrinsic band-gap absorption of ZnO due to the excitation of electrons. The presence of this peak indicates the successful synthesis of nanosized ZnO particles. Similar absorption peaks in the range of 360–380 nm have been widely reported for ZnO nanoparticles synthesized through biological synthesis methods.[35]
The optical band gap of ZnO nanoparticles was determined using the Tauc Plot derived from the Tauc relation:
$(\alpha h\nu)^n = A(h\nu - Eg)$ ----------(1)
where h is Planck's constant, ν is the photon frequency, α is the absorption coefficient, Eg is the band gap energy, and A is a proportionality constant. [36] The band gap energy was calculated by plotting $(\alpha h\nu)^2$ versus hν, as shown in Fig. 3(b). By extrapolating the linear portion of the curve to the energy axis, the band gap energy of the synthesized ZnO nanoparticles was determined to be 3.26 eV.[37]
The slight variation in band gap compared with bulk ZnO may be attributed to the quantum confinement effect, particle size variation, and surface defects present in the nanoparticles. These results confirm that the synthesized ZnO nanoparticles possess good optical properties and can be potentially used in applications such as photocatalysis,antibacterialactivity,andsensordevice

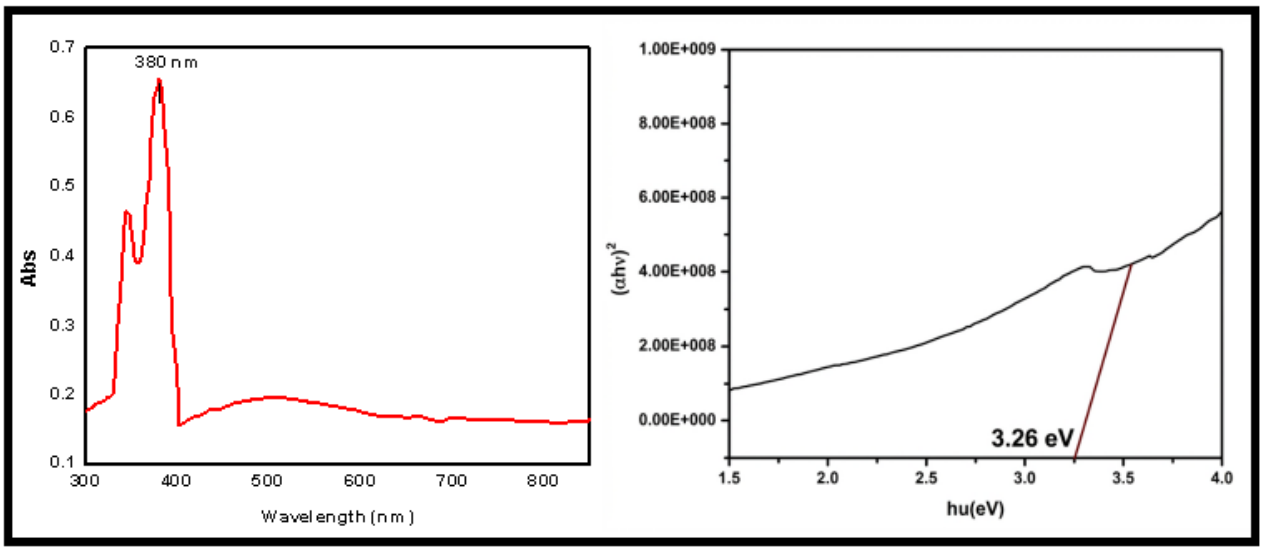

Fig.3 (a,b) - UV-Vis Spectrum of Zinc Oxide NPs & Tauc plot relation

5.2 XRD (X-ray Diffraction) Analysis)

REDVET - Revista electrónica de Veterinaria - ISSN 1695-7504
Vol 25, No. 2 (2024)
http://www.veterinaria.org
Article Received: 20.10.2024 Revised: 90.11.2024 Accepted: 08.12.2024

The X-ray diffraction (XRD) pattern of zinc oxide (ZnO) nanoparticles synthesized using *Herdmania pallida* extract is shown in Fig. The diffraction peaks were observed at 2θ = 31.7581°, 34.4832°, 36.6075°, and 47.2076°, which correspond to the Miller indices (100), (002), (101), and (102) respectively. These diffraction peaks confirm that the synthesized ZnO nanoparticles possess a hexagonal phase with a wurtzite crystal structure, which is in good agreement with the standard JCPDS card No. 89-7102. [38,39] The sharp and well-defined peaks indicate that the prepared ZnO nanoparticles exhibit good crystallinity, and the absence of additional peaks suggests that the synthesized nanoparticles are phase pure without detectable impurities.

Among the observed peaks, the (100) plane shows the highest intensity, indicating a strong preferential orientation of ZnO nanocrystals along this plane. The crystallite size of the ZnO nanoparticles was estimated using the Debye–Scherrer equation, given by:

$D = k\lambda / \beta \cos \theta$ ------- (1)

where D is the average crystallite size, k is the shape factor (0.94), λ is the X-ray wavelength (1.5421 Å), β is the full width at half maximum (FWHM) in radians, and θ is the Bragg angle. The average crystal size has been calculated from XRD analysis using the Debye–Scherrer equation, which in this study was approximately equal to ≈45 nm..[40]

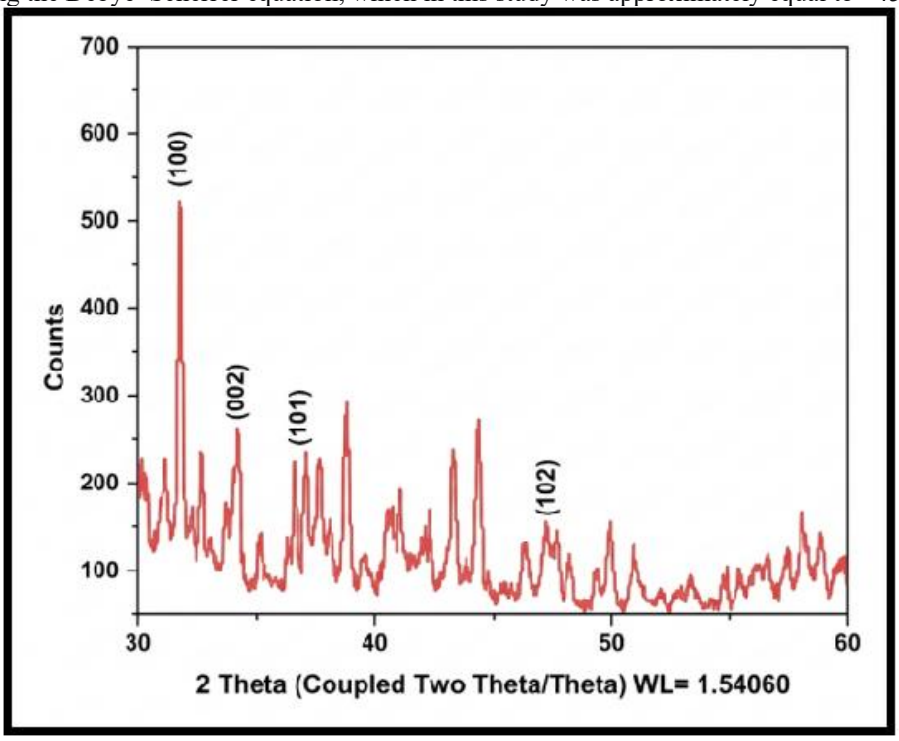

Fig. 4 XRD Analysis of ZnONPs

5.4 Scanning Electron Microscopy (SEM)

The morphology of the synthesized ZnO nanoparticles was examined using Scanning Electron Microscopy (SEM). The SEM images recorded at different magnifications (Fig. 5 a,b) reveal the formation of ZnO nanoparticles with irregular and agglomerated structures. The particles appear as clustered aggregates composed of smaller nanosized grains distributed across the surface.

In the SEM The higher magnification image with a 20 µm scale clearly shows rod-like and irregular nanostructures, suggesting that the nanoparticles are formed through nucleation and growth processes during biosynthesis.micrograph with a 50 µm scale, the particles appear densely packed with flake-like and granular structures, indicating the formation of crystalline ZnO particles. The SEM images further indicate that ZnO nanoparticles synthesized using *Herdmania pallida* extract exhibit different morphologies, including spherical and rod-like shapes with some degree of aggregation.[41] This variation in particle shape may be attributed to the presence of different biomolecules in the extract acting as reducing and capping agents, which influence the nucleation and growth of nanoparticles.[42] The observed aggregation may also result from the high surface energy of nanoparticles and interactions between particles during the drying process. the SEM analysis confirms the successful formation of ZnO nanoparticles with irregular, spherical, and rod-like aggregated morphology, which is commonly reported for biologically synthesized ZnO nanoparticles. The observed morphology also supports the structural results obtained from other characterization techniques.

REDVET - Revista electrónica de Veterinaria - ISSN 1695-7504
Vol 25, No. 2 (2024)
http://www.veterinaria.org
Article Received: 20.10.2024 Revised: 90.11.2024 Accepted: 08.12.2024

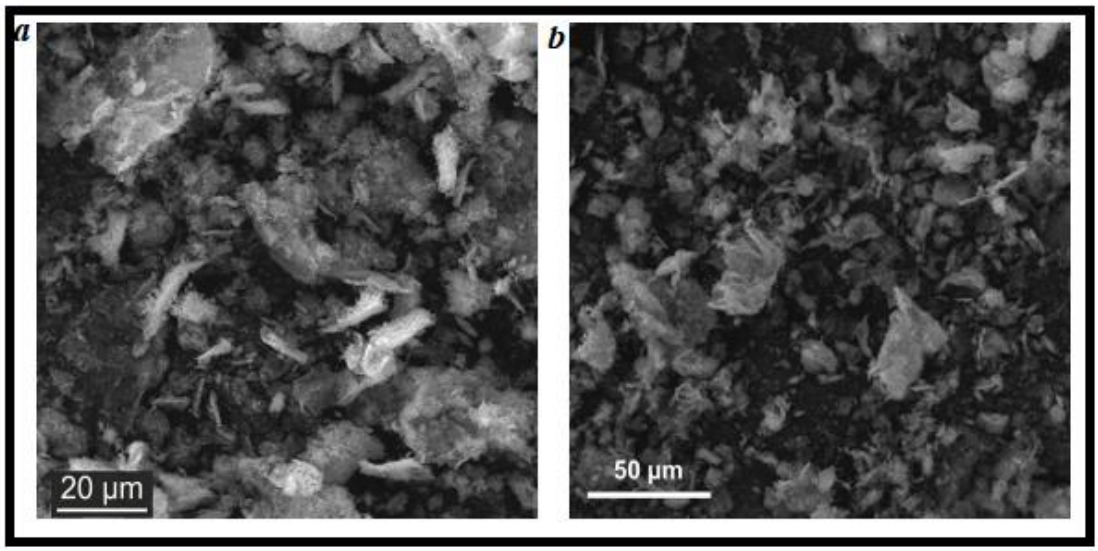

Fig. 5 (a,b): SEM Image of Zinc Oxide NPs

5.5 Energy Dispersive X-Ray Spectroscope (EDAX):

The elemental composition of the synthesized ZnO nanoparticles was analyzed using Energy Dispersive X-ray Analysis (EDAX). The EDAX spectrum (Fig. 6) confirms the presence of zinc (Zn) and oxygen (O) as the major elements, indicating the successful formation of ZnO nanoparticles. The spectrum shows a characteristic absorption peak of oxygen (O) at around 0.5 keV and prominent peaks of zinc (Zn) at approximately 1.0 keV and 8.68 keV, which confirms the presence of ZnO in the prepared sample [43].

The quantitative analysis reveals that oxygen (O) has a weight percentage of 44.43 wt% and an atomic percentage of 76.57 at%, while zinc (Zn) exhibits 55.57 wt% and 23.43 at%, respectively. The total normalized weight percentage of the detected elements is 100%, indicating the purity of the synthesized sample without the presence of significant impurity elements.The slightly higher atomic percentage of oxygen compared to zinc may be attributed to the surface adsorption of oxygen-containing biomolecules from the *Herdmania pallida* extract used during the green synthesis process. These biomolecules may act as reducing, capping, and stabilizing agents, which contribute to the formation and stabilization of ZnO nanoparticles.The obtained EDAX data are in good agreement with previously reported studies, which confirm that Zn and O are the main elemental components of ZnO nanoparticles synthesized using biological extracts [44]. Overall, the EDAX analysis clearly verifies the successful biosynthesis and elemental purity of the ZnO nanoparticles, supporting the results obtained from other characterization techniques such as XRD and SEM.

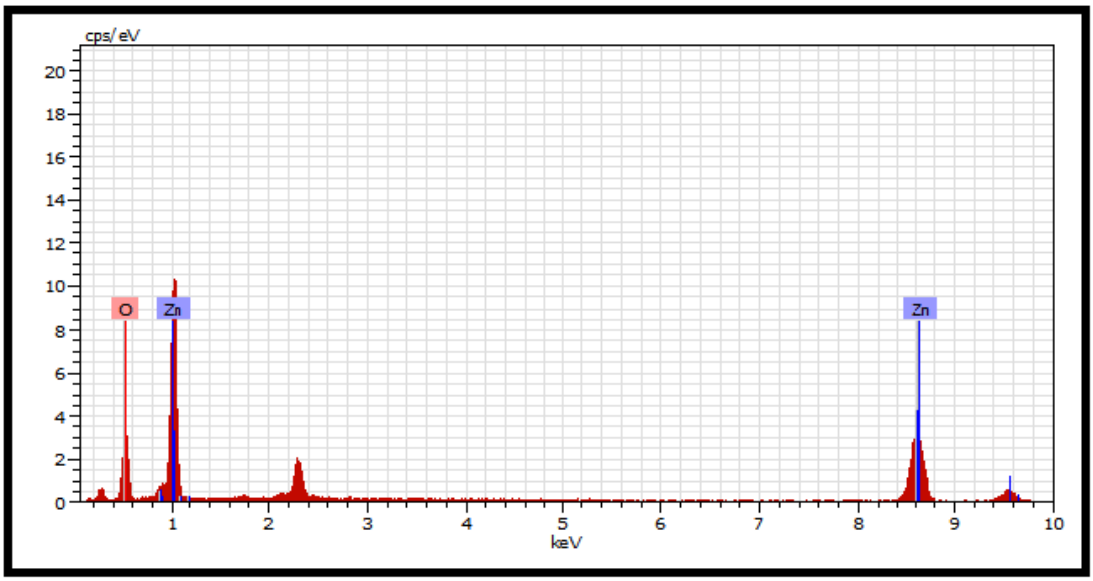

Fig.6. EADX Analysis of Zinc Oxide NPs

Table 1 ***EADX Analysis of Zinc Oxide NPs***

REDVET - Revista electrónica de Veterinaria - ISSN 1695-7504
Vol 25, No. 2 (2024)
http://www.veterinaria.org
Article Received: 20.10.2024 Revised: 90.11.2024 Accepted: 08.12.2024

Element	*AN*	*SERIES*	*Unn (Wt %)*	*C.Norm (Wt %)*	*C.Atom (at %)*	*1 Sigma (wt %)*
O	***8***	***K-series***	***36.66***	***44.43***	***76.57***	***6.28***
Zn	***30***	***K -series***	***45.85***	***55.57***	***23.43***	***1.25***
		Total	***82.51***	***100.00***	***100.00***	

5.3. Fourier Transform Infrared Radiation Spectroscopy (FTIR) Analysis

Fourier Transform Infrared Radiation Spectroscopy (FTIR, Nicolet iS5) was conducted in the spectral array from 400 to 3500 cm-^{1} for the prediction of major functional groups that may act as a capping, reducing, or stabilizing agent during nanosynthesis of ZnO NPs. FTIR spectroscopy was utilized to predict the surface adsorption of the functional groups present on the ZnO NPs. FTIR spectra of the ZnO NPs are in the spectral range of 400–3500 cm-^{1} , as shown in Figure 3. The absorption peaks were observed in the regions of 466 cm-^{1}, 673 cm-^{1}, 890 cm-^{1} , 1019 cm-^{1}, 1384 cm-^{1}, 1466 cm-^{1}, 1626 cm-^{1}, 2923 cm-^{1}, and 3434 cm-^{1}, respectively. A characteristic band predicted at 673 cm−1 and 466.95 cm -1 corresponds to it. The peak intensity at 890 represents the C-H of the aromatics, [45, 46] 1019 cm-^{1} corresponds to the C-O stretch , and 1466 cm-^{1} corresponds to the CN stretch of amide I in protein [47]. The peak at 1384 cm-^{1} suggests the presence of organic molecules or functional groups associated with specific chemical bonds. It could be related to C-H bending vibrations in aliphatic compounds [48], and 1626 cm-^{1} corresponds to the C=O stretch [49] , and 2923 cm-^{1} corresponds to the C-H stretch bond [50]. The peak at 3434 cm-^{1} corresponds to the OH group [51,52]. Zn-O stretching bond, as ZnO NPs were reported in the region of 650–400 cm-^{1} These results demonstrate the significant importance of biological molecules in ZnO NP fabrication.

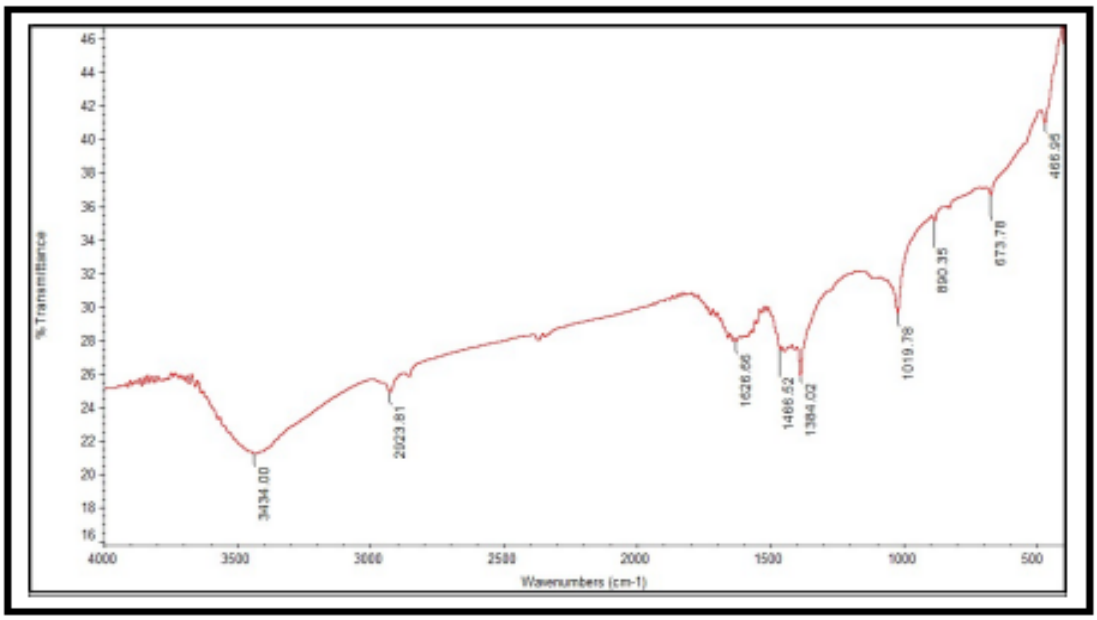

Fig. 7: IR spectrum of Herdmania pallida extract

5.4. Cyclic Voltammetry Analysis:

The representative CV curves for ZnO are shown in Fig. 8.{a} with different scan rates. The increased scan rate from 10 to 100 mV increases the redox peaks for ZnO samples. The CV curve shows a quasi-rectangular shape, indicating good capacitive behavior. These effects specify that the charge and discharge process of the ZnO pasted electrode displays good electrochemical reversibility of the electrodes. The oxidation and reduction peak currents are directly proportional to the scan rates, which means that the reaction is surface confined.Valuable information to categorize the process as diffusion-controlled or adsorption-controlled can be obtained by relating peak current and scan rate.Figure 8{b} shows the voltammetric behavior at differing scan rates in the range of 10–100 mV/s was studied using cyclic voltammetry. A plot of log current versus log scan rate was made to obtain a straight line indicating a completely diffusion-controlled [53] Additionally, the anodic peak potential shifted toward more positive values and the cathodic peak potential shifted toward more negative values as the scan rate increased, indicating quasi-reversible electron-transfer kinetics. These results demonstrate that the ZnO nanoparticles possess good electrochemical activity and allow efficient ion diffusion during the redox process.

REDVET - Revista electrónica de Veterinaria - ISSN 1695-7504
Vol 25, No. 2 (2024)
http://www.veterinaria.org
Article Received: 20.10.2024 Revised: 90.11.2024 Accepted: 08.12.2024

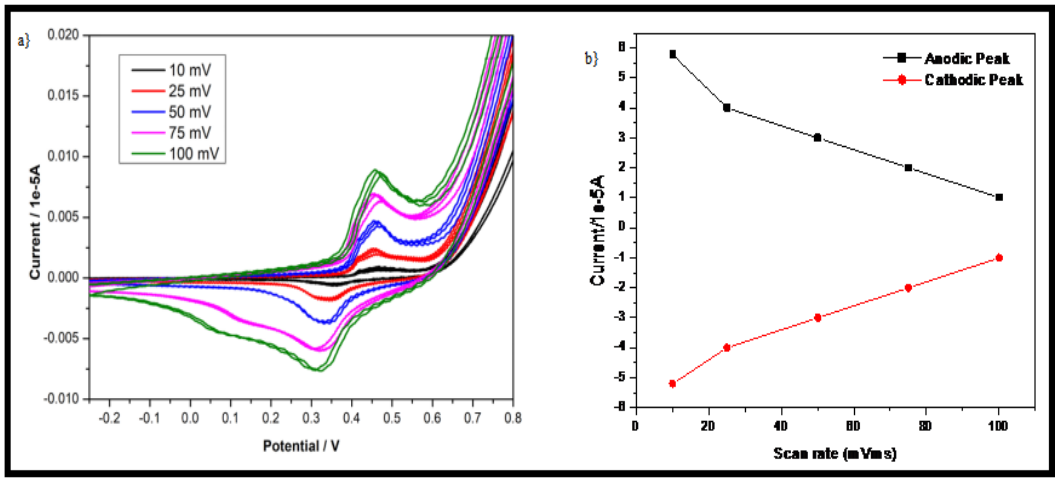

Fig. 8 (a) CV curves of ZnO particle &(b) calibration graph of current response vs.scan rate for the cathodic and anodic peak

5.5. Photocatalytic Activity:

The photocatalytic performance of ZnO nanostructures was investigated through the degradation of methylene blue (MB), a common organic pollutant dye. The degradation process was monitored by measuring the visible light absorbance of MB at λmax = 662 nm [54] at different irradiation time intervals under UV light, as shown in Fig. 10. The absorption spectra display a prominent peak around 660–670 nm, which corresponds to the characteristic absorption band of MB dye. A gradual decrease in the absorbance intensity with increasing irradiation time confirms the progressive degradation of the dye molecules, indicating the effective photocatalytic activity of the synthesized ZnO nanoparticles.

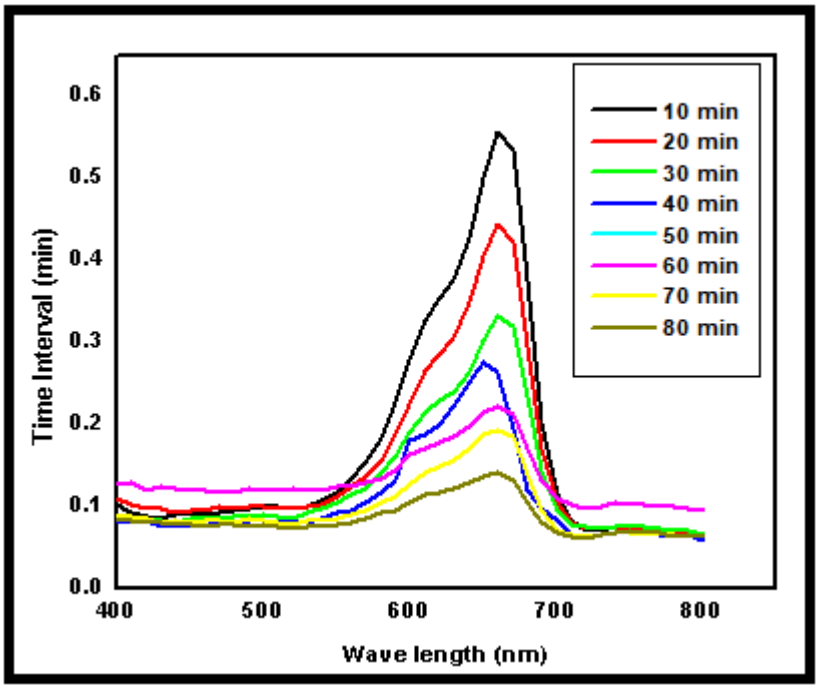

Fig. 9.Incubuation Time on Photocatalytic Activity

5.6.1 Pseudo-first-order kinetic

At the initial stage (10 min), the absorbance peak is relatively high, indicating a higher concentration of MB dye in the solution. As the irradiation time increases (20, 30, 40, 50, 60, 70, and 80 min), the absorbance intensity steadily decreases, demonstrating the continuous degradation of the dye in the presence of ZnO nanoparticles. The decline in absorbance occurs due to the photocatalytic activity of ZnO under UV irradiation. The photocatalytic degradation kinetics of MB is illustrated in Fig. 10(a). The degradation data were analyzed using the pseudo-first-order kinetic model, which can be expressed as:

$- \ln (A_o / A_t) = kt$

REDVET - Revista electrónica de Veterinaria - ISSN 1695-7504
Vol 25, No. 2 (2024)
http://www.veterinaria.org
Article Received: 20.10.2024 Revised: 90.11.2024 Accepted: 08.12.2024

where A_0 and A_t represent the initial absorbance and absorbance at time *t*, respectively, and k is the apparent rate constant. The plot of ln (A_t/A_0) versus time exhibited good linearity, confirming that the photocatalytic degradation follows pseudo-first-order kinetics. The degradation rate constant was calculated as k = 0.03047 min^{-1},[55] with a good linear correlation coefficient ($R^2 \approx 0.94557$), indicating efficient photocatalytic activity of the synthesized ZnO nanoparticles.

5.6.2.Degradation Efficiency:

The degradation efficiency increased progressively with increasing irradiation time, as shown in Fig. 10.(b) Initially, the degradation efficiency is relatively low due to limited interaction between the dye molecules and the catalyst surface. As the reaction proceeds, the degradation efficiency increases significantly because of the enhanced formation of reactive oxygen species and the availability of active catalytic sites.

Furthermore, the degradation efficiency was calculated using the following equation:

Degradation (%) = ($A_0 - At/ A_0$) × 100

The maximum degradation efficiency achieved in the present study was 77.58%, [56]demonstrating the strong photocatalytic capability of the biosynthesized ZnO nanoparticles., where ZnO nanoparticles synthesized using *Herdmania pallida* extract showed approximately 80% degradation of MB within two hours. The photocatalytic efficiency of nanoparticles is largely influenced by factors such as particle size, surface area, and the presence of structural defects, which enhance the generation and separation of charge carriers.[57,58] Therefore, the results of the present study confirm that the biosynthesized ZnO nanoparticles exhibit significant photocatalytic activity and hold potential for applications in wastewater treatment and environmental remediation.

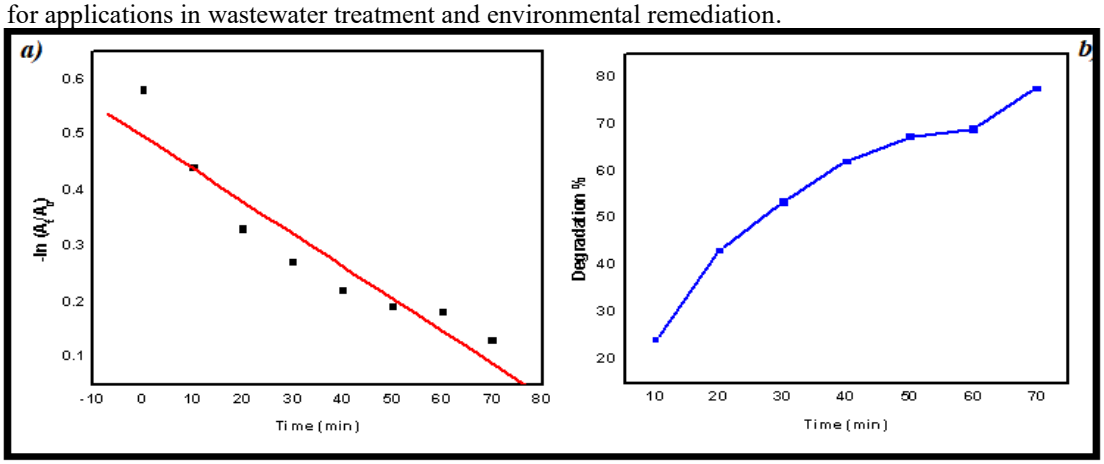

Fig. 10(a) Pseudo–first-order kinetics for MB by ZnO & Fig..10(b). Degradation % for MB by ZnO

5.6.3 Effect of dye concentration

The effect of the concentration of MB (50, 100, 150, and 200 ppm) in Fig. 11 was studied by keeping the catalyst in different concentrations.While increasing the dye concentration from 50 to 100 ppm, the rate of degradation also increases, but with further increase of concentration, the degradation rate decreases. This may be due to the inability of light to reach the catalyst surface at high dye concentrations [59].

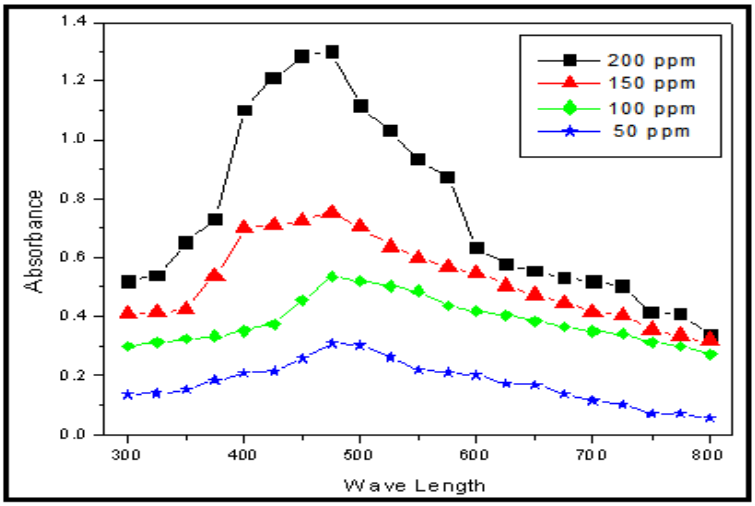

Fig. 11 Effect of Dye Concentration Using Photocatalytic Activity

REDVET - Revista electrónica de Veterinaria - ISSN 1695-7504
Vol 25, No. 2 (2024)
http://www.veterinaria.org
Article Received: 20.10.2024 Revised: 90.11.2024 Accepted: 08.12.2024

6.APPLICATION:

6.1.Antioxidant Activity of Synthesized Nanoparticles:

A. DPPH radical scavenging activity:

The antioxidant activity of ZnO nanoparticles synthesized using *Herdmania pallida* extract was evaluated and compared with the standard Ascorbic acid. The percentage of radical scavenging activity increased gradually with increasing concentration from 25–125 mg/mL.At 25 mg/mL, ZnO nanoparticles showed 29.76 ± 0.08% inhibition, whereas the standard showed 13.21 ± 0.11%. With increasing concentration, the scavenging activity of ZnO nanoparticles increased significantly to 79.21 ± 0.14% at 125 mg/mL, while ascorbic acid exhibited 66.52 ± 0.19% inhibition at the same concentration.The IC_{50} value represents the concentration required to inhibit 50% of free radicals. The IC_{50} value of ZnO nanoparticles was 63.42 mg/mL, whereas the IC_{50} value of ascorbic acid was 78.26 mg/mL. The lower IC_{50} value of ZnO nanoparticles indicates higher antioxidant potential compared with the standard.[60]The enhanced antioxidant activity may be attributed to the large surface area of ZnO nanoparticles and the presence of bioactive compounds from the *Herdmania pallida* extract, which can effectively donate electrons to neutralize free radicals. These results demonstrate that the biosynthesized ZnO nanoparticles possess significant free radical scavenging ability, suggesting their potential application in biomedical and pharmaceutical fields.

Table.2 A.Antioxidant Activity of ZnO NPs by DPPH radical scavenging activity:

Concentration mg/mL	ZnO	Ascorbic acid
25	29.76 ± 0.08	13.21 ± 0.11
50	42.70 ± 0.17	28.46 ± 0.09
75	56.58 ± 0.12	39.14 ± 0.18
100	68.32 ± 0.17	52.36 ± 0.24
125	79.21 ± 0.14	66.52 ± 0.19
IC_{50}	**63.42**	**78.26**

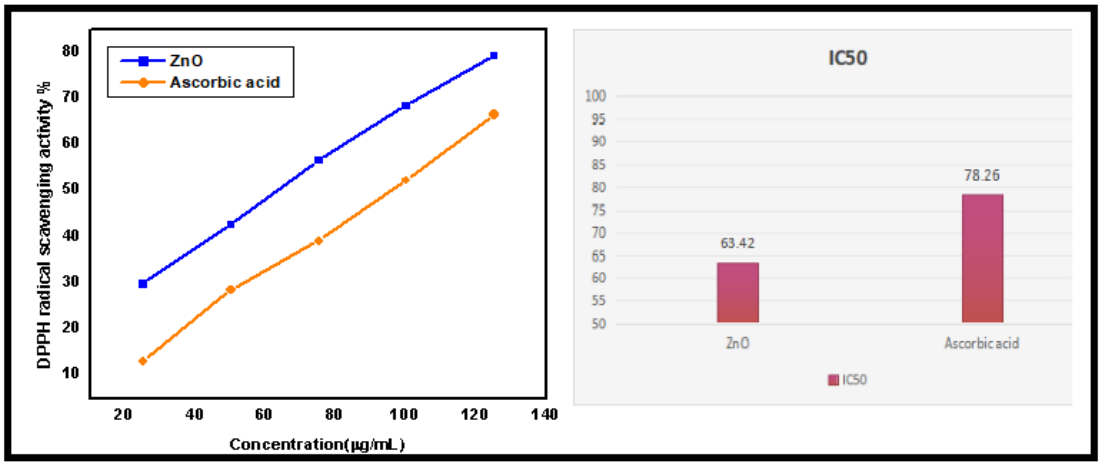

Fig. 12 DPPH Scavenging Assay Activity of ZnO

B. Hydrogen peroxide radical scavenging activity:

The hydrogen peroxide scavenging activity of ZnO nanoparticles synthesized using *Herdmania pallida* extract was evaluated and compared with the standard antioxidant Ascorbic acid. The scavenging activity increased progressively with increasing concentration (25–125 mg/mL), indicating a concentration-dependent antioxidant effect.At 25 mg/mL, ZnO nanoparticles showed 25.26 ± 0.09% inhibition, whereas ascorbic acid exhibited 12.14 ± 0.08% scavenging activity. With increasing concentration, the inhibition efficiency gradually increased. At the highest concentration (125 mg/mL), ZnO nanoparticles demonstrated 82.26 ± 0.12% scavenging activity, while ascorbic acid showed 63.24 ± 0.22%.The IC_{50} value, which represents the concentration required to scavenge 50% of hydrogen peroxide radicals, was calculated to be 66.35 mg/mL for ZnO nanoparticles and 71.26 mg/mL for ascorbic acid. The lower IC_{50} value of ZnO nanoparticles indicates higher hydrogen peroxide scavenging efficiency compared with the standard antioxidant.The enhanced activity may be attributed to the large surface area of ZnO nanoparticles and the presence of bioactive compounds from the *Herdmania pallida* extract, which facilitate electron transfer and neutralize reactive oxygen species such as H_2O_2. Hydrogen peroxide is a weak oxidizing agent but can generate highly reactive hydroxyl radicals in biological systems. Therefore, the ability of ZnO nanoparticles to effectively scavenge H_2O_2 suggests their potential role as protective antioxidant agents in biomedical applications.

REDVET - Revista electrónica de Veterinaria - ISSN 1695-7504
Vol 25, No. 2 (2024)
http://www.veterinaria.org
Article Received: 20.10.2024 Revised: 90.11.2024 Accepted: 08.12.2024

Table:3 B.Antioxidant Activity of ZnO NPs by H_2O_2 radical scavenging activity:

Concentration mg/mL	ZnO	Ascorbic acid
25	25.26 ± 0.09	12.14 ± 0.08
50	40.16 ± 0.17	25.26 ± 0.13
75	55.32 ± 0.11	38.28 ± 0.18
100	69.11 ± 0.14	46.72 ± 0.14
125	82.26 ± 0.12	63.24 ± 0.22
IC_{50}	**66.35**	**71.26**

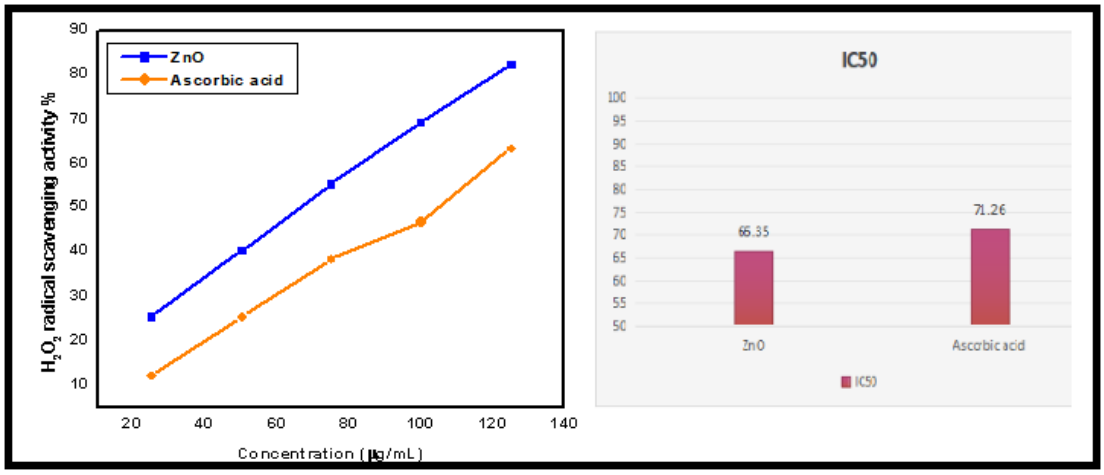

Fig. 13 H_2O_2 Scavenging Assay Activity of ZnO

6.1 Antibacterial Activity:

The antibacterial activity of ZnO nanoparticles was evaluated against *Escherichia coli*, *Staphylococcus aureus*, and *Pseudomonas aeruginosa* using the agar well diffusion method. The zone of inhibition was measured in millimeters (mm), and the results are presented in Table.4 .The synthesized ZnO nanoparticles exhibited a clear concentration-dependent antibacterial activity against all tested bacterial strains. The standard antibiotic (control) showed inhibition zones of 21 mm, 22 mm, and 23 mm against *E. coli*, *S. aureus*, and *P. aeruginosa*, respectively.

At lower concentration (50 µl), ZnO nanoparticles showed moderate inhibition with zones of 12 mm (*E. coli*), 10 mm (*S. aureus*), and 8 mm (*P. aeruginosa*). As the concentration increased, the antibacterial activity also increased gradually. At 100 µl and 150 µl, a steady rise in inhibition zones was observed, indicating enhanced interaction between nanoparticles and bacterial cells.The maximum antibacterial activity was recorded at 250 µl, with inhibition zones of 19 mm for *E. coli*, 14 mm for *S. aureus*, and 20 mm for *P. aeruginosa*. Among the tested organisms, *P. aeruginosa* showed the highest susceptibility, followed by *E. coli*, while *S. aureus* exhibited comparatively lower sensitivity.The higher susceptibility of Gram-negative bacteria (*E. coli* and *P. aeruginosa*) compared to Gram-positive bacteria (*S. aureus*) may be attributed to differences in cell wall structure. Gram-negative bacteria possess a thinner peptidoglycan layer, which facilitates easier penetration of ZnO nanoparticles, whereas Gram-positive bacteria have a thicker cell wall that restricts nanoparticle entry.

Table:4 Antibacterial Activity of ZnO NPs:

ZnO	Bacteria		
Inhibition zone (mm)	*E.Coli*	*S.aureus*	*P.aeruginosa*
Abs	21	22	23
50 µl	12	10	8
100 µl	13	11	11
150 µl	13	12	13
200 µl	14	13	15
250 µl	19	14	20

REDVET - Revista electrónica de Veterinaria - ISSN 1695-7504
Vol 25, No. 2 (2024)
http://www.veterinaria.org
Article Received: 20.10.2024 Revised: 90.11.2024 Accepted: 08.12.2024

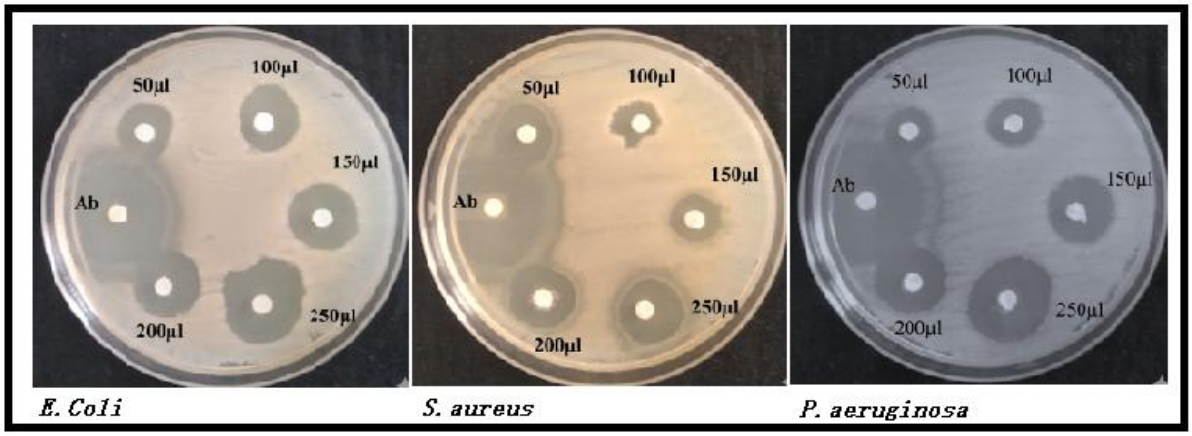

Fig.14. Antibacterial Activity of ZnO Np's

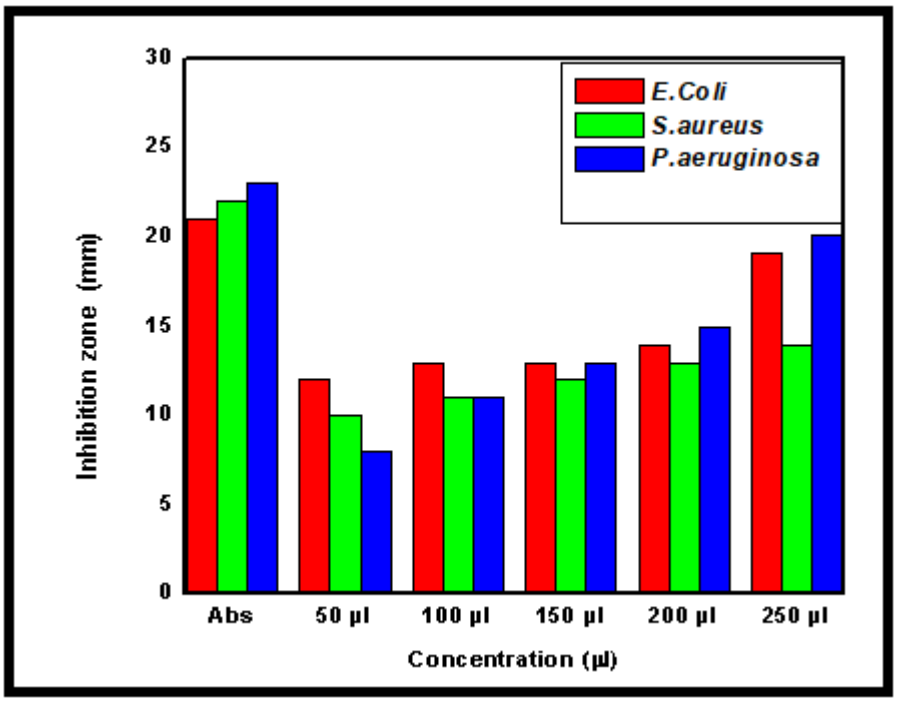

Fig.15 Zone of inhibition graph against bacterial strains

7. Conclusion:

In the present study, Zinc Oxide (ZnO) nanoparticles were successfully biosynthesized using Herdmania pallida extract through an eco-friendly and cost-effective green synthesis approach. The synthesized nanoparticles were characterized using UV–Visible spectroscopy, XRD, SEM, EDAX, FTIR, and cyclic voltammetry analyses, which confirmed their successful formation, crystalline nature, purity, surface morphology, functional groups, and excellent electrochemical behavior. The ZnO nanoparticles exhibited a characteristic absorption peak at 380 nm with a band gap energy of 3.26 eV and possessed a hexagonal wurtzite crystal structure with an average crystallite size of approximately 45 nm. Morphological studies revealed irregular, spherical, and rod-like nanostructures, while FTIR analysis confirmed the involvement of biomolecules in nanoparticle stabilization and capping.

Furthermore, the synthesized ZnO nanoparticles demonstrated significant photocatalytic activity toward methylene blue dye degradation, achieving a maximum degradation efficiency of 77.58%, indicating their potential application in wastewater treatment and environmental remediation. The nanoparticles also exhibited remarkable antioxidant activity with efficient free radical and hydrogen peroxide scavenging ability, along with strong antibacterial activity against both Gram-positive and Gram-negative bacterial strains. Overall, the findings of this study highlight that biosynthesized ZnO nanoparticles possess excellent optical, structural, electrochemical, photocatalytic, antioxidant, and antibacterial properties, making them promising candidates for biomedical, environmental, and nanotechnological applications.

ACKNOWLEDGMENT:

I express my sincere gratitude to Dr.S.Sankaravadivu for their guidance and support throughout this research work.I also thank and acknowledge the PG & Research Department of Chemistry,A.P.C.Mahalaxmi College for Women,Thoothukudi,for providing laboratoryf or synthesis nanoparticles and study for photocatalytic degradation,UV & FTIR Study from V.O.Chidambaram college PG & Research Department of Chemistry,Thoothukudi.Tamilnadu, XRD and Cyclic voltammetry study Avinashlingam Institute for the Home Science and Higher education for Women,Coimbatore,Tamilnadu. and Gandhigram Rural Institute,Dindigul,Tamilnadu,India. Study for SEM & EDAX.,.Antioxidant activity study from BIOmelTez Research & Development Pvt Ltd,Kanyakumari..Antibacterial activity study from Dr.G.Arunkumar,Kamaraj College Thoothukudi.Tamilnadu.

Conflicts of Interest:
The authors declare no conflict of Interest.

10 . REFERENCE:

1. Albrecht, Matthew A., Cameron W. Evans, and Colin L. Raston. "Green chemistry and the health implications of nanoparticles." *Green chemistry* 8, no. 5 (2006): 417-432.
2. Ebadi, Mojgan, Mohammad Reza Zolfaghari, Seyyed Soheil Aghaei, Mohsen Zargar, Morvarid Shafiei, Hossein Shahbani Zahiri, and Kambiz Akbari Noghabi. "A bio-inspired strategy for the synthesis of zinc oxide nanoparticles (ZnO NPs) using the cell extract of cyanobacterium Nostoc sp. EA03: from biological function to toxicity evaluation." *RSC advances* 9, no. 41 (2019): 23508-23525.
3. Mahmoud, Alaa El Din, and Manal Fawzy. "Nanosensors and nanobiosensors for monitoring the environmental pollutants." In *Waste recycling technologies for nanomaterials manufacturing*, pp. 229-246. Cham: Springer International Publishing, 2021.
4. Geonmonond, Rafael S., Anderson GM DA Silva, and Pedro HC Camargo. "Controlled synthesis of noble metal nanomaterials: motivation, principles, and opportunities in nanocatalysis." *Anais da Academia Brasileira de Ciências* 90, no. 1 Suppl 1 (2018): 719-744.
5. Harant, H. "Les Tuniciers comestibies." *Atti del* 11 (1951): 1-3.
6. Delsuc, Frédéric, Henner Brinkmann, Daniel Chourrout, and Hervé Philippe. "Tunicates and not cephalochordates are the closest living relatives of vertebrates." *Nature* 439, no. 7079 (2006): 965-968.
7. Bone, Q_, C. Carre, and P. Chang. "Tunicate feeding filters." *Journal of the Marine Biological Association of the United Kingdom* 83, no. 5 (2003): 907-919.
8. Jacobi, Yuval, Gitai Yahel, and Noa Shenkar. "Efficient filtration of micron and submicron particles by ascidians from oligotrophic waters." *Limnology and Oceanography* 63, no. S1 (2018): S267-S279.
9. Jiang, A., Z. Yu, and C. H. Wang. "Bioaccumulation of cadmium in the ascidian Styela clava (Herdman 1881)." *African Journal of Marine Science* 31, no. 3 (2009): 289-295.
10. Treberg, Jason R., Joy E. Stacey, and William R. Driedzic. "Vanadium accumulation in ascidian coelomic cells is associated with enhanced pentose phosphate pathway capacity but not overall aerobic or anaerobic metabolism." *Comparative Biochemistry and Physiology Part B: Biochemistry and Molecular Biology* 161, no. 4 (2012): 323-330.
11. Shenkar, Noa, and Billie J. Swalla. "Global diversity of Ascidiacea." *Plos one* 6, no. 6 (2011): e20657.
12. Novak, L., S. Lopez-Legentil, E. Sieradzki, and N. Shenkar. "Rapid establishment of the non-indigenous ascidian Styela plicata and its associated bacteria in marinas and fishing harbors along the Mediterranean coast of Israel." *Mediterranean Marine Science* 18, no. 2 (2017): 324-331.
13. Raja, BT Antony. "BAY OF BENGAL PROGRAMME BOB P/WP/37."
14. Meenakshi, V. K., M. Paripooranaselvi, S. Sankaravadivu, S. Gomathy, and K. P. Chamundeeswari. "Immunomodulatory activity of Phallusia nigra Savigny, 1816 against S-180." *Int J Curr Microbiol Appl Sci* 2, no. 8 (2013): 286-295.
15. Mohammed, Hamdoon A., Salmin K. Alshalmani, and Awad Giumma Abdellatif. "Antioxidant and quantitative estimation of phenolic and flavonoids of three halophytic plants growing in Libya." *J. Pharmacog. Photochem* 2, no. 3 (2013): 89-94.
16. Pandit, Chetan, Arpita Roy, Suresh Ghotekar, Ameer Khusro, Mohammad Nazmul Islam, Talha Bin Emran, Siok Ee Lam, Mayeen Uddin Khandaker, and David Andrew Bradley. "Biological agents for synthesis of nanoparticles and their applications." *Journal of King Saud University-Science* 34, no. 3 (2022): 101869.
17. Theodore, Louis. *Nanotechnology: basic calculations for engineers and scientists*. John Wiley & Sons, 2006.
18. Wang, Xilong, Jialong Lu, Minggang Xu, and Baoshan Xing. "Sorption of pyrene by regular and nanoscaled metal oxide particles: influence of adsorbed organic matter." *Environmental science & technology* 42, no. 19 (2008): 7267-7272.
19. Dagdeviren, Canan, Suk-Won Hwang, Yewang Su, Stanley Kim, Huanyu Cheng, Onur Gur, Ryan Haney, Fiorenzo G. Omenetto, Yonggang Huang, and John A. Rogers. "Transient, biocompatible electronics and energy harvesters based on ZnO." *small* 9, no. 20 (2013): 3398-3404.

20. Amornpitoksuk, P., S. Suwanboon, S. Sangkanu, A. Sukhoom, J. Wudtipan, K. Srijan, and S. Kaewtaro. "Synthesis, photocatalytic and antibacterial activities of ZnO particles modified by diblock copolymer." *Powder technology* 212, no. 3 (2011): 432-438.
21. Penn, Sharron G., Lin He, and Michael J. Natan. "Nanoparticles for bioanalysis." *Current opinion in chemical biology* 7, no. 5 (2003): 609-615.
22. Andleeb, Anisa, Aneeta Andleeb, Salman Asghar, Gouhar Zaman, Muhammad Tariq, Azra Mehmood, Muhammad Nadeem, Christophe Hano, Jose M. Lorenzo, and Bilal Haider Abbasi. "A systematic review of biosynthesized metallic nanoparticles as a promising anti-cancer-strategy." *Cancers* 13, no. 11 (2021): 2818.
23. Rouhi, Jalal, Shahrom Mahmud, Nima Naderi, CH Raymond Ooi, and Mohamad Rusop Mahmood. "Physical properties of fish gelatin-based bio-nanocomposite films incorporated with ZnO nanorods." *Nanoscale research letters* 8, no. 1 (2013): 364.
24. Baxter, Jason B., and Eray S. Aydil. "Nanowire-based dye-sensitized solar cells." *Applied physics letters* 86, no. 5 (2005).
25. Sharma, Jyoti Laxmi, Veena Dhayal, and Rakesh Kumar Sharma. "White-rot fungus mediated green synthesis of zinc oxide nanoparticles and their impregnation on cellulose to develop environmental friendly antimicrobial fibers." *3 Biotech* 11, no. 6 (2021): 269.
26. Rauf, Mohd Ahmar, Mohammad Oves, Fawad Ur Rehman, Abdur Rauf Khan, and Nazim Husain. "Bougainvillea flower extract mediated zinc oxide's nanomaterials for antimicrobial and anticancer activity." *Biomedicine & Pharmacotherapy* 116 (2019): 108983.
27. Safawo, Tura, B. V. Sandeep, Sudhakar Pola, and Aschalew Tadesse. "Synthesis and characterization of zinc oxide nanoparticles using tuber extract of anchote (Coccinia abyssinica (Lam.) Cong.) for antimicrobial and antioxidant activity assessment." *OpenNano* 3 (2018): 56-63.
28. Soltanian, Sara, Mahboubeh Sheikhbahaei, Neda Mohamadi, Athareh Pabarja, Maryam Fekri Soofi Abadi, and Mohammad Hossein Mohammadi Tahroudi. "Biosynthesis of zinc oxide nanoparticles using Hertia intermedia and evaluation of its cytotoxic and antimicrobial activities." *BioNanoScience* 11, no. 2 (2021): 245-255.
29. Abdo, Abdullah M., Amr Fouda, Ahmed M. Eid, Nayer M. Fahmy, Ahmed M. Elsayed, Ahmed Mohamed Aly Khalil, Othman M. Alzahrani, Atef F. Ahmed, and Amal M. Soliman. "Green synthesis of Zinc Oxide Nanoparticles (ZnO-NPs) by Pseudomonas aeruginosa and their activity against pathogenic microbes and common house mosquito, Culex pipiens." *Materials* 14, no. 22 (2021): 6983.
30. Nagaswarupa, H. P., M. Mylarappa, D. M. K. Siddeswara, KR Vishnu Mahesh, and N. Raghavendra. "Fabrication and hierarchical structure of ZnO nano particle using green fuels: cyclic voltammetry and impedance analysis." *Materials Today: Proceedings* 5, no. 10 (2018): 22547-22553.
31. Pai, Shraddha, H. Sridevi, Thivaharan Varadavenkatesan, Ramesh Vinayagam, and Raja Selvaraj. "Photocatalytic zinc oxide nanoparticles synthesis using Peltophorum pterocarpum leaf extract and their characterization." *Optik* 185 (2019): 248-255.
32. Blois, Marsden S. "Antioxidant determinations by the use of a stable free radical." *Nature* 181, no. 4617 (1958): 1199-1200.
33. Revathi, S. L., S. Kumar, V. Sudarshana Deepa, and S. Kumar. "Antimicrobial activity of A. serpyllifolia (Rohl. Ex. Vahl) Wright." *Int. J. Pharma. Sci. Health Care* 1 (2014): 2249-2257.
34. Bauer, A. W., Kirby, W. M., Sherris, J. C., & Turck, M. (1966). Antibiotic susceptibility testing by a standardized single disk method. *American journal of clinical pathology*, *45*(4_ts), 493-496.
35. Hirose, E., Ohtsuka, K., Ishikura, M., & Maruyama, T. (2004). Ultraviolet absorption in ascidian tunic and ascidian-Prochloron symbiosis. *Journal of the Marine Biological Association of the United Kingdom*, *84*(4), 789-794.
36. .Viezbicke, B. D., Patel, S., Davis, B. E., & Birnie III, D. P. (2015). Evaluation of the Tauc method for optical absorption edge determination: ZnO thin films as a model system. *physica status solidi (b)*, *252*(8), 1700-1710.
37. Kumar, V., Kaushal, S., & Singh, Y. (2025). Biogenic synthesis of zinc oxide nanoparticles using cell-free extract of Spirogyra crassa (Kütz.) Kütz for sustainable biomedical and environmental applications. *New Journal of Chemistry*, *49*(37), 16145-16159.
38. Sivasankarapillai, V. S., Krishnamoorthy, N., Eldesoky, G. E., Wabaidur, S. M., Islam, M. A., Dhanusuraman, R., & Ponnusamy, V. K. (2023). One-pot green synthesis of ZnO nanoparticles using Scoparia Dulcis plant extract for antimicrobial and antioxidant activities. *Applied Nanoscience*, *13*(9), 6093-6103.
39. El-Belely, E. F., Farag, M. M., Said, H. A., Amin, A. S., Azab, E., Gobouri, A. A., & Fouda, A. (2021). Green synthesis of zinc oxide nanoparticles (ZnO-NPs) using Arthrospira platensis (Class: Cyanophyceae) and evaluation of their biomedical activities. *Nanomaterials*, *11*(1), 95.
40. .El-Belely, E. F., Farag, M. M., Said, H. A., Amin, A. S., Azab, E., Gobouri, A. A., & Fouda, A. (2021). Green synthesis of zinc oxide nanoparticles (ZnO-NPs) using Arthrospira platensis (Class: Cyanophyceae) and evaluation of their biomedical activities. *Nanomaterials*, *11*(1), 95.
41. Meer, B., Andleeb, A., Iqbal, J., Ashraf, H., Meer, K., Ali, J. S., ... & Abbasi, B. H. (2022). Bio-assisted synthesis and characterization of zinc oxide nanoparticles from Lepidium sativum and their potent antioxidant, antibacterial and anticancer activities. *Biomolecules*, *12*(6), 855.

42. Priya, D. S., Sankaravadivu, S., Sudha, S., & Christy, H. K. S. (2021). Synthesis and characterisation of silver nanoparticles using phallusia nigra. *Annals of RSCB*, *25*(4), 12948-12957.
43. Vinayagam, R., Pai, S., Varadavenkatesan, T., Pugazhendhi, A., & Selvaraj, R. (2023). Characterization and photocatalytic activity of ZnO nanoflowers synthesized using Bridelia retusa leaf extract. *Applied Nanoscience*, *13*(1), 493-502.
44. Anjali, K. P., Sangeetha, B. M., Raghunathan, R., Devi, G., & Dutta, S. (2021). Seaweed mediated fabrication of zinc oxide nanoparticles and their antibacterial, antifungal and anticancer applications. *ChemistrySelect*, *6*(4), 647-656.
45. Nazir, Saher, Mehreen Zaka, Muhammad Adil, Bilal Haider Abbasi, and Christophe Hano. "Synthesis, characterisation and bactericidal effect of ZnO nanoparticles via chemical and bio-assisted (Silybum marianum in vitro plantlets and callus extract) methods: a comparative study." *IET nanobiotechnology* 12, no. 5 (2018): 604-608.
46. Meer, Bisma, Anisa Andleeb, Junaid Iqbal, Hajra Ashraf, Kushif Meer, Joham Sarfraz Ali, Samantha Drouet et al. "Bio-assisted synthesis and characterization of zinc oxide nanoparticles from Lepidium sativum and their potent antioxidant, antibacterial and anticancer activities." *Biomolecules* 12, no. 6 (2022): 855.
47. Yedurkar, Snehal, Chandra Maurya, and Prakash Mahanwar. "Biosynthesis of zinc oxide nanoparticles using ixora coccinea leaf extract—a green approach." *Open Journal of Synthesis Theory and Applications* 5, no. 1 (2016): 1-14.
48. Kalaba, Mohamed H., Gamal M. El-Sherbiny, Emad A. Ewais, Osama M. Darwesh, and Saad A. Moghannem. "Green synthesis of zinc oxide nanoparticles (ZnO-NPs) by Streptomyces baarnensis and its active metabolite (Ka): a promising combination against multidrug-resistant ESKAPE pathogens and cytotoxicity." *BMC microbiology* 24, no. 1 (2024): 254.
49. Fouda, Amr, Ahmed M. Eid, Ayman Abdelkareem, Hanan A. Said, Ehab F. El-Belely, Dalal Hussien M. Alkhalifah, Khalid S. Alshallash, and Saad El-Din Hassan. "Phyco-synthesized zinc oxide nanoparticles using marine macroalgae, Ulva fasciata Delile, characterization, antibacterial activity, photocatalysis, and tanning wastewater treatment." *Catalysts* 12, no. 7 (2022): 756.
50. Mahamuni, Pranjali P., Pooja M. Patil, Maruti J. Dhanavade, Manohar V. Badiger, Prem G. Shadija, Abhishek C. Lokhande, and Raghvendra A. Bohara. "Synthesis and characterization of zinc oxide nanoparticles by using polyol chemistry for their antimicrobial and antibiofilm activity." *Biochemistry and biophysics reports* 17 (2019): 71-80.
51. Naiel, Bassant, Manal Fawzy, Marwa Waseem A. Halmy, and Alaa El Din Mahmoud. "Green synthesis of zinc oxide nanoparticles using Sea Lavender (Limonium pruinosum L. Chaz.) extract: characterization, evaluation of anti-skin cancer, antimicrobial and antioxidant potentials." *Scientific Reports* 12, no. 1 (2022): 20370.
52. Smith, Janice Gorzynski. "Mass spectrometry and infrared spectroscopy." *Organic chemistry* (2011): 463-488.
53. Saleem, Qasar, Sammia Shahid, Abdur Rahim, Majed A. Bajaber, Sana Mansoor, Mohsin Javed, Shahid Iqbal et al. "A highly explicit electrochemical biosensor for catechol detection in real samples based on copper-polypyrrole." *RSC advances* 13, no. 20 (2023): 13443-13455
54. Kappadan, S., Gebreab, T. W., Thomas, S., & Kalarikkal, N. (2016). Tetragonal BaTiO3 nanoparticles: An efficient photocatalyst for the degradation of organic pollutants. *Materials Science in semiconductor processing*, *51*, 42-47.
55. Pandimurugan, R., & Thambidurai, S. (2016). Novel seaweed capped ZnO nanoparticles for effective dye photodegradation and antibacterial activity. *Advanced Powder Technology*, *27*(4), 1062-1072.
56. Nava, O. J., Luque, P. A., Gómez-Gutiérrez, C. M., Vilchis-Nestor, A. R., Castro-Beltrán, A., Mota-González, M. L., & Olivas, A. (2017). Influence of Camellia sinensis extract on Zinc Oxide nanoparticle green synthesis. *Journal of Molecular Structure*, *1134*, 121-125.
57. Ngoepe, N. M., Mbita, Z., Mathipa, M., Mketo, N., Ntsendwana, B., & Hintsho-Mbita, N. C. (2018). Biogenic synthesis of ZnO nanoparticles using Monsonia burkeana for use in photocatalytic, antibacterial and anticancer applications. *Ceramics International*, *44*(14), 16999-17006.
58. . Liang, H., Tai, X., Du, Z., & Yin, Y. (2020). Enhanced photocatalytic activity of ZnO sensitized by carbon quantum dots and application in phenol wastewater. *Optical Materials*, *100*, 109674.
59. Sivakumar, P., G. K. Gaurav Kumar, P. Sivakumar, and S. Renganathan. "Synthesis and characterization of ZnS-Ag nanoballs and its application in photocatalytic dye degradation under visible light." *Journal of Nanostructure in Chemistry* 4, no. 3 (2014): 107.
60. Abdelbaky, A. S., Abd El-Mageed, T. A., Babalghith, A. O., Selim, S., & Mohamed, A. M. (2022). Green synthesis and characterization of ZnO nanoparticles using Pelargonium odoratissimum (L.) aqueous leaf extract and their antioxidant, antibacterial and anti-inflammatory activities. *Antioxidants*, *11*(8), 1444.